FEBS Letters 586 (2012) 3858–3864

journal homepage: www.FEBSLetters.org

Structural insight into the interaction of ADP-ribose with the PARP WWE domains

Fahu He [a], Kengo Tsuda [a], Mari Takahashi [a], Kanako Kuwasako [a], Takaho Terada [a], Mikako Shirouzu [a], Satoru Watanabe [a], Takanori Kigawa [a,b], Naohiro Kobayashi [a], Peter Güntert [c,d], Shigeyuki Yokoyama [a,*], Yutaka Muto [a,*]

[a] RIKEN Systems and Structural Biology Center, 1-7-22 Suehiro-cho, Tsurumi-ku, Yokohama 230-0045, Kanagawa, Japan
[b] Tokyo Institute of Technology, 4259 Nagatsuda-cho, Midori-ku, Yokohama 226-8502, Kanagawa, Japan
[c] Tatsuo Miyazawa Memorial Program, RIKEN Genomic Sciences Center, Yokohama 230-0045, Kanagawa, Japan
[d] Institute of Biophysical Chemistry, Center for Biomolecular Magnetic Resonance, and Frankfurt Institute of Advanced Studies, Goethe University Frankfurt, Max-von-Laue-Str. 9, 60438 Frankfurt am Main, Germany

ARTICLE INFO

Article history:
Received 19 June 2012
Revised 30 August 2012
Accepted 12 September 2012
Available online 22 September 2012

Edited by Christian Griesinger

Keywords:
WWE domain
NMR spectroscopy
Solution structure
ADP-ribose

ABSTRACT

The WWE domain is often identified in proteins associated with ubiquitination or poly-ADP-ribosylation. Structural information about WWE domains has been obtained for the ubiquitination-related proteins, such as Deltex and RNF146, but not yet for the poly-ADP-ribose polymerases (PARPs). Here we determined the solution structures of the WWE domains from PARP11 and PARP14, and compared them with that of the RNF146 WWE domain. NMR perturbation experiments revealed the specific differences in their ADP-ribose recognition modes that correlated with their individual biological activities. The present structural information sheds light on the ADP-ribose recognition modes by the PARP WWE domains.

1. Introduction

The WWE domain was termed according to its conserved Trp and Glu residues, and has been found in two functional subfamilies [1]. One is associated with ubiquitination and the other with poly ADP-ribose polymerases (PARPs). The first structural information about a WWE domain was obtained for the Deltex protein, a ubiquitin E3 ligase targeting the ankyrin repeats of the Notch receptor [2]. Each of the two tandemly-linked Deltex WWE domains adopts a β1–β2–α1–β3–β4–β5–β6 topology, and they intra-molecularly interact with each other to stabilize their binding to the ankyrin repeats on the surface of these domains.

In addition, a recent X-ray crystallographic study revealed that the WWE domain of the RNF146 protein, which is a ubiquitin E3 ligase for poly-ADP-ribosylated axin, preferentially binds to the iso-ADP-ribose moiety (Fig. 1A) on the top of the β-barrel structure [3]. Thus, structural information about the WWE domains that are involved in ubiquitination has been reported so far. However, no structural information is available for the WWE domains from PARPs, and the binding preference of the PARP WWE domains to ADP-ribose moieties was not revealed in previous surface plasmon resonance (SPR) experiments with several WWE domains and a poly ADP-ribose chain [3].

The binding preferences of the WWE domains of PARPs for ADP-ribose derivatives are interesting subjects, because only the ADP-ribose moiety appears at the terminus of the mono ADP-ribosylated chain, instead of the iso-ADP-ribose moiety (Fig. 1A), and it could be the enzymatic target of some PARPs [4]. Here, we report the solution structures of the WWE domains of the PARP subfamily members PARP11 and PARP14, and we compared the new structures with that of RNF146 (Fig. 1B) to reveal the differences in their interactions with derivatives of ADP-ribose.

2. Materials and methods

2.1. Protein sample preparation

The protein sample used for the NMR experiments were constructed for the WWE domains of mouse RNF146, human PARP11 and mouse PARP14 (corresponding to residues 83–179, 15–105 and 1542–1618, respectively).

Abbreviations: HSQC, heteronuclear single quantum coherence; NOE, nuclear Overhauser enhancement; NOESY, NOE spectroscopy; PARP, poly-ADP-ribose polymerase; ITC, isothermal titration calorimetry

* Corresponding authors. Fax: +81 45 503 9195.
E-mail addresses: yokoyama@riken.jp (S. Yokoyama), ymuto@gsc.riken.jp (Y. Muto).

0014-5793/$36.00
http://dx.doi.org/10.1016/j.febslet.2012.09.009

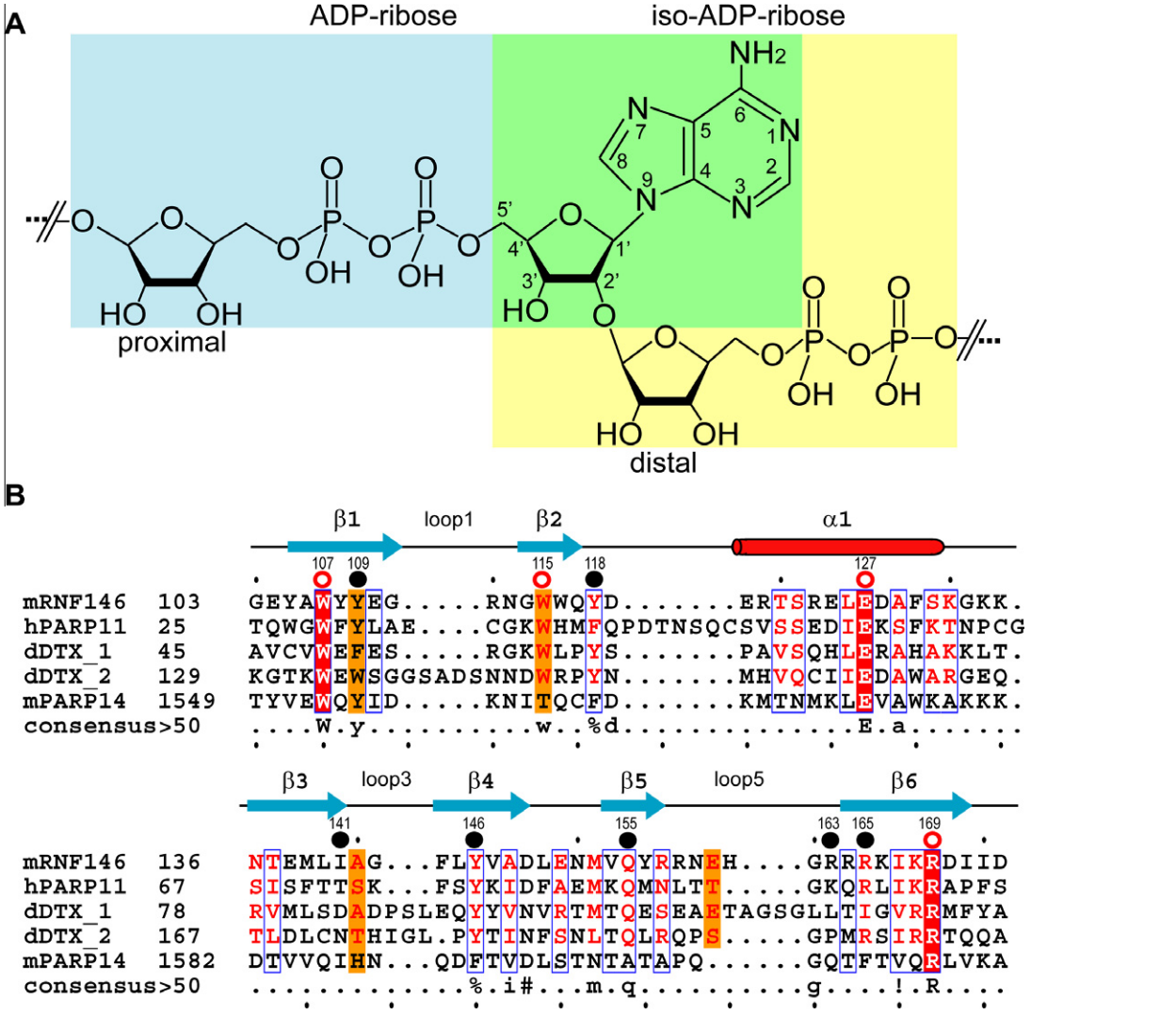

Fig. 1. (A) Structures of the ADP-ribose and iso-ADP-ribose moieties in the poly-ADP-ribose chain. (B) Structure-based sequence alignment of WWE domains. Secondary structure elements of the RNF146 WWE domain are shown on the top. The highly conserved Trp and Glu residues are marked by open red circles for the RNF146 WWE domain. The closed black circles indicate the amino acid residues involved in the recognition of the ADP-ribose moiety.

These WWE domains were synthesized by a cell-free protein synthesis system [5,6]. For the structure determination, a sample of 1.1 mM uniformly ^{13}C- and ^{15}N-labeled protein was prepared in 20 mM ^{2}H-Tris–HCl buffer, containing 100 mM NaCl, 1 mM dithiothreitol (DTT), and 0.02 % (w/v) NaN_3, with the addition of D_2O to 10% v/v, at pH 7.0. ADP-ribose, ADP, ATP, adenine, and NAD+ were purchased from Sigma.

2.2. NMR spectroscopy and resonance assignments

NMR experiments were performed at 25 °C on 600 and 800 MHz spectrometers (Bruker DRX600 and AV800), equipped with *xyz*-pulsed field gradients. Backbone and side chain assignments were obtained by standard triple resonance experiments [7]. All assignments were checked for consistency with 3D ^{15}N- and ^{13}C-edited NOESY-HSQC spectra. 3D NOESY spectra were recorded with mixing times of 80 ms. For the assignment of ATP in complex with the RNF146 WWE domain, 2D filtered NOESY spectra with mixing times of 80 and 150 ms, and 2D filtered TOCSY spectra were used [8]. The NMR data were processed with the program NMRPipe [9]. Spectra were analyzed with the programs NMRView [10], KUJIRA [11], and SPARKY (T. D. Goddard and D. G. Kneller, SPARKY 3, University of California, San Francisco).

2.3. Structure calculations

The three-dimensional structures were determined by combined automated NOESY cross peak assignment and structure calculation with torsion angle dynamics, implemented in the CYANA program [12,13]. Restraints for the backbone torsion angles ϕ and ψ were determined by a chemical shift database analysis with the program TALOS [14]. For the determination of the three-dimensional structures of the RNF146 WWE domain-ATP complex, NMR measurements were performed with mixtures of the RNF146 WWE domain and ATP at molar ratios of 1:0.5, 1:1, and 1:2. The intermolecular protein-ATP NOEs were assigned automatically and inspected manually, using the 3D NOESY-HSQC spectra and the 2D filtered NOESY spectra with mixing times of 80 and 150 ms, respectively. Structure calculations were performed in the same manner as for the free WWE domains. The 20 structures from the CYANA calculation were subjected to restrained energy refinement with the program AMBER9, using the Generalized Born

model [15]. PROCHECK-NMR was used to validate the final structures [16]. Structure figures were prepared with the program MOLMOL [17].

The 20 energy-refined conformers of the free WWE domains from PARP11, PARP14 and RNF146, and the RNF146 WWE domain in complex with ATP, have been deposited in the Protein Data Bank (PDB entries 2DK6, 1X4R, 1URJ, and 2RSF, respectively). The chemical shift assignments have been deposited in the BioMagResBank database, with the accession codes 11500, 11501, 11499, and 11472, respectively.

2.4. NMR titration experiments

For the chemical shift titration experiments, five derivatives of ADP-ribose (ADP-ribose, ADP, ATP, adenine, and NAD+) were dissolved in the same buffer as the protein samples, to make 7 mM solutions. 2D [^{1}H,^{15}N]-HSQC spectra were recorded while increasing the ligand concentration relative to that of the WWE domain (0.2 mM), to a final 1:2 or 1:5 ratio of the WWE domain to the ligands.

2.5. ITC measurements

ITC measurements were performed at 25 °C, using a Microcal (Amherst, MA) VP-ITC calorimeter. Samples were buffered with 20 mM Tris–HCl (pH 7.0) containing 100 mM NaCl, and were thoroughly degassed before use. First, a 2.0 ml aliquot of a ~50 μM WWE domain solution was placed in the cell chamber. The five different ligand solutions (ADP-ribose, ADP, ATP, adenine, and NAD+), at a ~60-fold higher concentration, were then injected into it. The heat generated due to dilution of the titrant was used as the reference for the analysis. The data were analyzed with the Microcal ORIGIN software, using a binding model that assumes a single site of interaction.

2.6. Molecular modeling

Model structures of WWE domains of RNF146 and PARP11 in complex with ADP-ribose and ATP were generated using Molmol and AMBER9 programs. For the PARP11 WWE domain in complex with ATP, the protein coordinate of RNF146 in the complex structure with ATP was replaced with that of the lowest energy-minimization structure of the PARP11 WWE domain. For RNF146 and PARP11 WWE domains in complex with ADP-ribose, the ATP coordinates in the complex structure were replaced with those of ADP-ribose to fulfill the NMR perturbation results, respectively. These template structures were then refined in 1500-step energy minimizations in vacuum to avoid bad steric contacts using AMBER9 program. The parameter for ADP-ribose was generated using Antechamber module, and AMBER ff99SB– and GAFF force fields were applied in calculations for energy minimization.

3. Results and discussion

3.1. Solution structures of the WWE domains from PARP11, PARP14, and RNF146

We solved the solution structures of the WWE domains from RNF146, PARP11, and PARP14. The final 20 energy-minimized conformers that represent the solution structures of the WWE domains are well defined and show excellent agreement with the experimental data (Table S1).

The RNF146 WWE domain exhibits a β1–β2–α1–β3–β4–β5–β6 topology in solution (Figs. 2A and S1A), in agreement with the X-ray structure of the RNF146 WWE domain (PDB entry 1UJR) [3]. The six β-strands form a β-barrel-like structure in solution. The top of the β-barrel-like structure is open to the solvent and adorned with three loops (loop1, loop3, and loop5). As viewed from above, the hydrophobic side chains of W116 (β2 strand) and F144 (loop3) are exposed to the solvent, as doorkeepers for the top pocket. Y109 (β1 strand), I141 (β3 strand) and Y146 (β4 strand) form the inner surface of the pocket. Y118 (β2 strand) and Q155 (β5 strand) are located at the bottom of the pocket (Fig. 2A).

The domain architectures of the PARP11 and PARP14 WWE domains resemble that of the RNF146 WWE domain. On the other hand, several unique structural features were identified in each of the PARP WWE domains. In the PARP11 WWE domain (Figs. 2B and S1B), an additional flexible hairpin structure was identified between the β2 strand and the 1 helix (spanning residues P43 to C49, and hereafter referred to as the L1 loop). Therefore, the PARP11 WWE domain adopts the fold with the β1–β2–L1–α1–β3–β4–β5–β6 topology. In spite of its specific L1 loop structure, the PARP11 WWE domain has the characteristic open pocket at the top of the β-barrel-like structure (Fig. 2D) and contains the crucial aromatic and Gln residues (Y31, F41, Y77, and Q87), corresponding to Y109, Y118, Y146, and Q155 of the RNF146 WWE domain (Fig. 2A and B).

As described above, the domain architecture of the PARP14 WWE domain is closely related to that of RNF146 (Figs. 2C and S1C). However, the β3 strand protrudes into the top pocket of the PARP14 WWE domain, and seems to cover the pocket (Fig. 2C and D).

3.2. ADP-ribose moiety binding preferences of WWE domains

As reported previously [3,18], poly-ADP-ribose is a putative target of the WWE domain, and the RNF146 WWE domain preferred iso-ADP-ribose over ADP-ribose. However, the iso-ADP-ribose moiety does not appear in the mono ADP-ribose modification, which could be one of the targets of PARPs. Thus, it is conceivable that the binding preferences for the ADP-ribose chains are different between the PARP and RNF146 WWE domains. Therefore, we examined the binding preferences of the PARP11, PARP14, and RNF146 WWE domains for several ADP-ribose derivatives (ADP, ATP, ADP-ribose, adenine, and NAD+) by NMR titration and ITC experiments.

The 2D [^{1}H, ^{15}N]-HSQC titration experiment for the RNF146 WWE domain revealed that ADP and ATP exert more significant perturbations on the RNF146 WWE domain than ADP-ribose (Figs. S2 and S3). Correspondingly, ITC experiments revealed the affinities of ADP and ATP to the WWE domain, with K_d values of 325 μM and 141 μM, respectively (Table 1). In comparison to the binding of ADP and ATP, that of ADP-ribose is significantly weaker (K_d value of 1.7 mM by ITC) (Table 1 and Fig. S4). Simultaneously, neither adenine nor NAD+ interacted with the RNF146 WWE domain, although NAD+ is a precursor of poly ADP-ribosylation (Table 1 and Fig. S4). Therefore, we concluded that the ADP moiety is an essential binding unit for the RNF146 WWE domain, but the additional proximal ribose reduced the interaction with the RNF146 WWE domain.

In the NMR titration experiments, the PARP11 WWE domain also exhibited clear-cut chemical shift changes at the top area of the β-barrel-like structure upon ATP binding (Figs. S5A and S6A). The characteristic L1 loop of the PARP11 WWE domain was also affected. In the case of the PARP11 WWE domain, the addition of ADP-ribose caused a similar perturbation pattern as that observed with the addition of ATP (Fig. S6). However, the magnitudes of the chemical shift changes for each amino acid residue were larger than those for ATP, and some resonances disappeared (Figs. S5A, S5B, and S6). Actually, the ITC experiments revealed that the PARP11 WWE domain binds more tightly to ADP-ribose than to ADP and ATP (K_d values for ADP-ribose, ADP, and ATP are

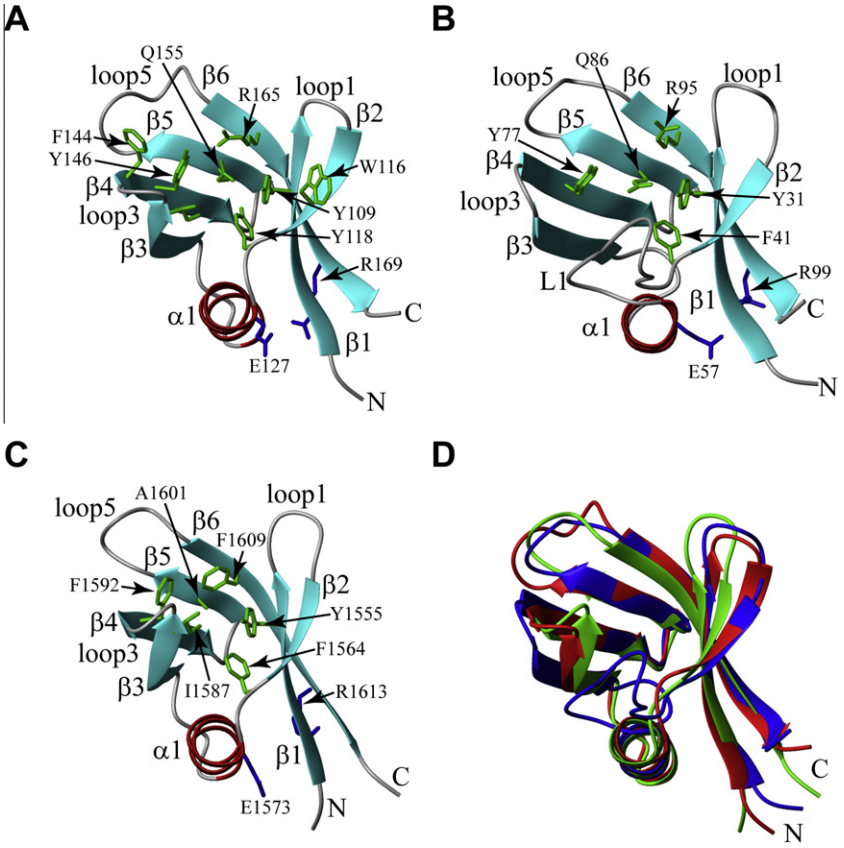

Fig. 2. Ribbon representations of the WWE domains from (A) RNF146, (B) PARP11, and (C) PARP14. The well converged regions (RNF146: residues 103–173, PARP11: residues 25–103, and PARP14: residues 1549–1617) are presented. The β-strands and α-helical structures are shown in cyan and red, respectively. The side chains of the highly conserved residues among the WWE domains are shown in green. (D) Superposition of the structures of the WWE domains of RNF146 (red), PARP11 (blue), and PARP14 (green).

Table 1
Binding affinities of the RNF146 and PARP11 WWE domains for several ADP-ribose derivatives.

Protein	Ligand	K_d
RNF146 WWE	Adenine	Not detected
RNF146 WWE	ATP	141 ± 2 μM
RNF146 WWE	ADP	326 ± 5 μM
RNF146 WWE	ADP-ribose	1712 ± 53 μM
RNF146 WWE	NAD+	Not detected
PARP11 WWE	ATP	9434 ± 186 μM
PARP11 WWE	ADP	>1 M
PARP11 WWE	ADP-ribose	400 ± 2 μM
PARP11 WWE	NAD+	>1 M

400 μM, larger than 1 M, and over 9 mM, respectively), in contrast to the case of the RNF146 WWE domain (Table 1 and Fig. S7). However, similar to the case of the RNF146 WWE domain, NAD + is not a good target molecule for the PARP11 WWE domain (K_d value for NAD + is larger than 1 M).

In the case of the PARP14 WWE domain, we could not observe any chemical shift changes in the 2D [^{1}H, ^{15}N]-HSQC spectra, even upon the addition of ATP (data not shown) (Fig. 1B).

3.3. Complex structure of the RNF146 WWE domain and ATP

In order to rationalize the results of the NMR titration experiment, we solved the solution structure of the RNF146 WWE domain in complex with ATP, because the RNF146 WWE domain exhibited the strongest binding activity for ATP among the WWE domains in our study.

In the complex structure, the adenine moiety fits well into the hydrophobic pocket composed of Y109, I141 and Y146 (Fig. 3A and 3B). The N6 amino group of adenine interacts with the hydroxyl oxygen of Y118 and the $O^{\varepsilon 1}$ atom of Q155 in the pocket (Fig. S8). Simultaneously, the N7 atom of ATP forms a hydrogen bond with the $H^{\varepsilon 2}$ protons of Q155. Furthermore, the O4′ of the sugar moiety of ATP interacts with the hydroxyl proton of Y146, as also observed in the previous X-ray structure [3].

We could not obtain structural information for the location of the ATP pyrophosphate group by NOESY experiments. In the chemical shift perturbation experiments, however, the backbone amide proton resonance of R163 shifted strongly upon the addition of ADP. In addition, those of R157 and R164 are affected by the ATP addition. This suggested that the pyrophosphate groups of ADP/ATP interact mainly with R163, and slightly with R157, for favorable electrostatic interactions, as depicted in the modeled structure in Figs. 3B and 4A.

3.4. Terminal ADP-ribose is not a suitable target for the RNF146 WWE domain

In order to compare the binding modes of the RNF146 WWE domain with ATP/ADP and ADP-ribose, we carefully examined the NMR titration results. The region spanning from F83 to M153 exhibited similar perturbation patterns for ADP/ATP and ADP-ribose (Figs. S3A, B and C). By changing the vertical scale of the perturbation results for ADP-ribose, we could superimpose

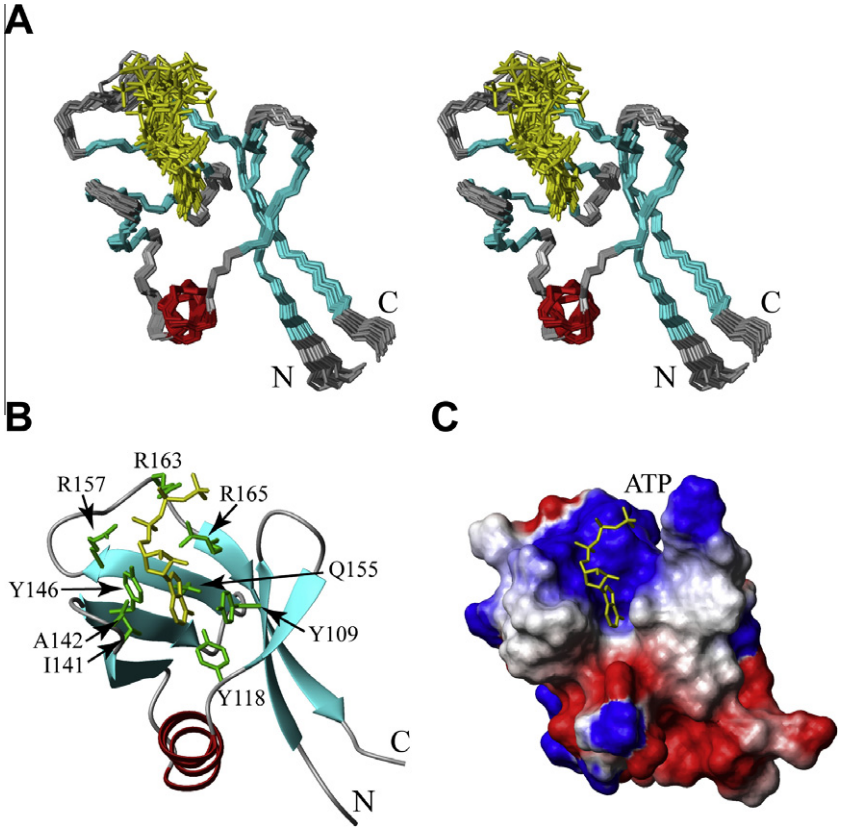

Fig. 3. (A) Stereoview of the backbone traces of the 20 solution structure conformers of the RNF146 WWE domain in the complex with ATP. (B) Lowest-energy solution structure of the RNF146 WWE domain-ATP complex, in a ribbon representation with interacting residues. (C) Electrostatic surface potential of the RNF146 WWE domain in complex with ATP.

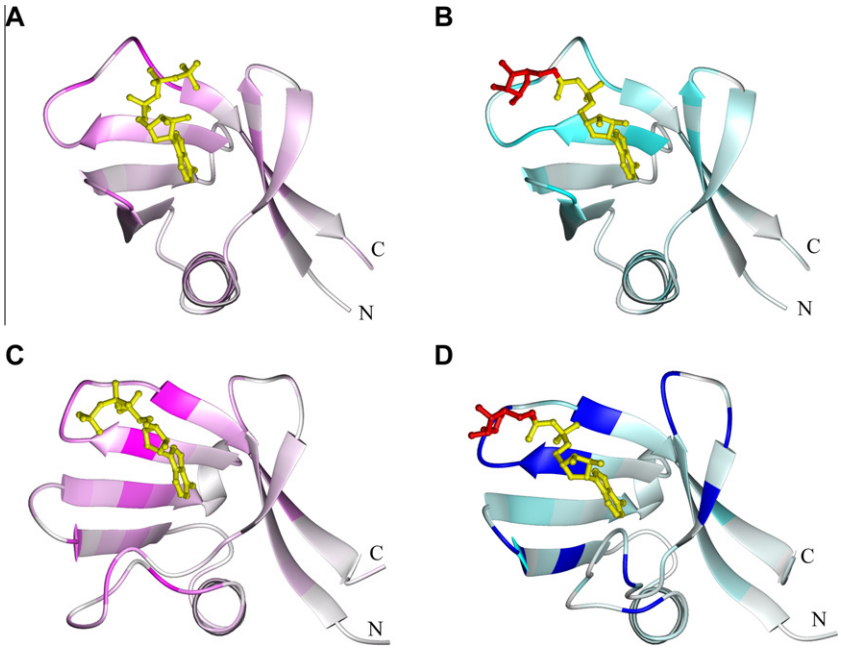

Fig. 4. (A) ATP and (B) ADP-ribose NMR titration results, mapped on the RNF146 WWE domain structure. (C) ATP and (D) ADP-ribose titration results, mapped on model structures of their complexes with the PARP11 WWE domain. The residues are colored with a gradient according to the amplitude of their chemical shift changes.

the perturbation pattern for this region, which revealed significant differences in loop5 between them (Fig. S9A and B). Namely, upon the addition of ADP/ATP, the amide-proton resonance of R163 is strongly affected. However, upon the addition of ADP-ribose, the effect on R163 is suppressed (Fig. S9), and the effect on the residues around R157 is increased. This implies that the proximal ribose

attachment to the phosphate group inhibits the suitable orientation of the pyrophosphate group for the interaction with R163, which reduces the binding to the ADP-ribose. A previous study revealed that the RNF146 WWE domain binds tightly to the iso-ADP ribose [3]. Thus, the presence of the distal ribose directly attached to the adenosine sugar moiety appears to be important for the RNF146 WWE domain to overcome the negative influence of the proximal ribose on binding to the poly-ADP-ribose chain, implying that the RNF146 WWE domain could not bind to the mono-ADP-ribose chain effectively.

3.5. The PARP11 WWE domain binds to the ADP ribose moiety, unlike the RNF146 WWE domain

We further examined the NMR titration results for the interactions of the PARP11 WWE domain with ATP and ADP-ribose (Fig. S5A and B). On the basis of the complex structure of the RNF146 WWE domain with ATP and the chemical shift perturbations, we built a model for the complex structure of the PARP11 WWE domain (Fig. 4C). In the modeled complex structure, the L1 loop contacts and recognizes the adenine base, instead of T72 on the β3-strand (corresponding to I141 of the RNF146 WWE domain).

The PARP11 WWE domain possesses a positively charged amino acid residue (K93) at the position corresponding to R163 in the RNF146 WWE domain. We actually observed a slight chemical shift change for the K93 resonance. However, T90 and T91 showed rather larger chemical shift changes, among the residues in loop5. The perturbation experiment suggested that the pyrophosphate group of ATP could reach the amino acid residues, including T90 and T91, and interact with them (Fig 4C).

Upon the addition of ADP-ribose, the signals of several amino acid residues around T90 and T91 disappeared. In contrast, the chemical shift change of K93 was small in comparison (Fig. S6). This suggested that the recognition of the pyrophosphate groups of ATP and ADP-ribose by the PARP11 WWE domain is mediated by the amino acid residues at the tip of loop5 (Fig. 4C and D), and that the proximal ribose is favorable for the extension of the pyrophosphate group to the tip of loop5 and for the recognition of ADP-ribose.

NMR titration experiments revealed that the PARP14 WWE domain could not bind to ATP. Although various hydrophobic amino acid residues that could recognize the adenosine moiety are somewhat conserved between the PARP14 and RNF146 WWE domains (Fig. 1B), the position corresponding to Q155 of the RNF146 WWE domain, which plays a crucial role in the recognition of the adenine base, is replaced with an Ala residue (A1601 in the PARP14 WWE domain). In addition, the hydrophobic pocket at the top of the β-barrel-like structure is covered with the β3-strand, and the side chain of I1587 (corresponding to I141 of RNF146) occupies the putative space for the adenine moiety (Fig. 2C). The PARP14 protein contains macro domains that could specifically recognize the ADP-ribose, apart from the WWE domain (complex structure, PDB entry 3Q6Z). Therefore, it is possible that the intrinsic activity of the PARP14 WWE domain has been gradually replaced with those of the macro domains.

3.6. Comparison with the ADP-ribose binding modes of other recognition domains

Other protein modules that interact with poly-ADP-ribose chains also exhibit diverse preferences. The first PBZ domain of APFL (aprataxin and PNK-like factor) recognizes iso-ADP-ribose [19,20]. In the complex, the adenine moiety is sandwiched by the exposed aromatic side chains of two Tyr residues (Y381 and Y386), and the distal ribose is expected to interact with the well-conserved Arg residue (R387) in the PBZ domain (Fig. S10A).

In contrast, the macro domain of macroH2A1.1 recognizes ADP-ribose. The carboxyl side chain of an Asp residue (D203) and the amide proton of the following Ile residue (I204) could hydrogen bond with the adenine moiety in the ditch formed near the N-terminus of the first α-helix. The ribose and pyrophosphate group fit well into the pocket formed by the two loop regions (G314-N316 and G223-G224). As a result, the macro domain specifically recognizes the terminal ADP-ribose moiety of the poly-ADP-ribose chain [21–23] (Fig. S10B).

In the present study, we revealed that the RNF146 and PARP11 WWE domains commonly have an adenosine recognition site (Fig. 3A). However, the proximal ribose that is linked to the phosphate group exerts different effects between them. The PARP11 WWE domain could recognize the terminal ADP-ribose, which lacks the distal ribose, in the poly-ADP-ribose. Thus, it is reasonable for the PARP11 WWE domain to exhibit an affinity for ADP-ribose. On the other hand, the RNF146 WWE domain preferentially binds to the iso-ADP-ribose moiety, which appears in the poly-ADP-ribose chain on the target protein. The present structural study suggested that loop5 of these WWE domains plays an important role in the different specificities between RNF146 and PARP11.

Acknowledgments

We are grateful to Dr. Yoshihide Hayashizaki (RIKEN OSC) for FANTOM clone (4933409B01). We are also grateful to Yasuko Tomo, Masaomi Ikari, Takeshi Nagira, Naoko Akimoto, Yukiko, Kinoshita-Sakaguchi, Yuki Kamewari-Hayami, Kazushige Katsura, Noboru Ohsawa and Tomoko Nishizaki for the sample preparation. This work was supported by the RIKEN Structural Genomics/Proteomics Initiative (RSGI), the National Project on Protein Structural and Functional Analyses of the Ministry of Education, Culture, Sports, Science and Technology of Japan (MEXT). P.G. acknowledges financial support by the Lichtenberg program of the Volkswagen Foundation and by the Japan Society for the Promotion of Science (JSPS).

Appendix A. Supplementary data

Supplementary data associated with this article can be found, in the online version, at http://dx.doi.org/10.1016/j.febslet.2012.09.009.

References

[1] Aravind, L. (2001) The WWE domain: a common interaction module in protein ubiquitination and ADP ribosylation. Trends Biochem. Sci. 26, 273–275.
[2] Zweifel, M.E., Leahy, D.J. and Barrick, D. (2005) Structure and Notch receptor binding of the tandem WWE domain of Deltex. Structure 13, 1599–1611.
[3] Wang, Z., Michaud, G.A., Cheng, Z., Zhang, Y., Hinds, T.R., Fan, E., Cong, F. and Xu, W. (2012) Recognition of the iso-ADP-ribose moiety in poly(ADP-ribose) by WWE domains suggests a general mechanism for poly(ADP-ribosyl)ation-dependent ubiquitination. Genes Dev. 26, 235–240.
[4] Gibson, B.A. and Kraus, W.L. (2012) New insight into the molecular and cellular functions of poly(ADP-ribose) and PARPs. Nat. Rev. Mol. Cell Biol. 13, 411–424.
[5] Matsuda, T. et al. (2007) Improving cell-free protein synthesis for stable-isotope labeling. J. Biomol. NMR 37, 225–229.
[6] Kigawa, T., Yabuki, T., Matsuda, N., Matsuda, T., Nakajima, R., Tanaka, A. and Yokoyama, S. (2004) Preparation of *Escherichia coli* cell extract for highly productive cell-free protein expression. J. Struct. Funct. Genomics 5, 63–68.
[7] Clore, G.M. and Gronenborn, A.M. (1994) Multidimensional heteronuclear nuclear magnetic resonance of proteins. Methods Enzymol. 239, 349–363.
[8] Peterson, R.D., Theimer, C.A., Wu, H. and Feigon, J. (2004) New applications of 2D filtered/edited NOESY for assignment and structure elucidation of RNA and RNA-protein complexes. J. Biomol. NMR 28, 59–67.
[9] Delaglio, F., Grzesiek, S., Vuister, G.W., Zhu, G., Pfeifer, J. and Bax, A. (1995) NMRPipe: a multidimensional spectral processing system based on UNIX pipes. J. Biomol. NMR 6, 277–293.
[10] Johnson, B.A. (2004) Using NMRView to visualize and analyze the NMR spectra of macromolecules. Methods Mol. Biol. 278, 313–352.

[11] Kobayashi, N., Iwahara, J., Koshiba, S., Tomizawa, T., Tochio, N., Güntert, P., Kigawa, T. and Yokoyama, S. (2007) KUJIRA, a package of integrated modules for systematic and interactive analysis of NMR data directed to high-throughput NMR structure studies. J. Biomol. NMR 39, 31–52.
[12] Güntert, P., Mumenthaler, C. and Wüthrich, K. (1997) Torsion angle dynamics for NMR structure calculation with the new program DYANA. J. Mol. Biol. 273, 283–298.
[13] Güntert, P. (2009) Automated structure determination from NMR spectra. Eur. Biophys. J. 38, 129–143.
[14] Cornilescu, G., Delaglio, F. and Bax, A. (1999) Protein backbone angle restraints from searching a database for chemical shift and sequence homology. J. Biomol. NMR 13, 289–302.
[15] Case, D.A. et al. (2005) The Amber biomolecular simulation programs. J. Comput. Chem. 26, 1668–1688.
[16] Laskowski, R.A., Rullmann, J.A., MacArthur, M.W., Kaptein, R. and Thornton, J.M. (1996) AQUA and PROCHECK-NMR: programs for checking the quality of protein structures solved by NMR. J. Biomol. NMR 8, 477–486.
[17] Koradi, R., Billeter, M. and Wüthrich, K. (1996) MOLMOL: a program for display and analysis of macromolecular structures. J. Mol. Graph. 14 (51–5), 29–32.
[18] Zhang, Y. et al. (2011) RNF146 is a poly(ADP-ribose)-directed E3 ligase that regulates axin degradation and Wnt signalling. Nat. Cell Biol. 13, 623–629.
[19] Eustermann, S., Brockmann, C., Mehrotra, P.V., Yang, J.C., Loakes, D., West, S.C., Ahel, I. and Neuhaus, D. (2010) Solution structures of the two PBZ domains from human APLF and their interaction with poly(ADP-ribose). Nat. Struct. Mol. Biol. 17, 241–243.
[20] Li, G.Y., McCulloch, R.D., Fenton, A.L., Cheung, M., Meng, L., Ikura, M. and Koch, C.A. (2010) Structure and identification of ADP-ribose recognition motifs of APLF and role in the DNA damage response. Proc. Natl. Acad. Sci. U S A 107, 9129–9134.
[21] Timinszky, G. et al. (2009) A macrodomain-containing histone rearranges chromatin upon sensing PARP1 activation. Nat. Struct. Mol. Biol. 16, 923–929.
[22] Malet, H. et al. (2009) The crystal structures of Chikungunya and Venezuelan equine encephalitis virus nsP3 macro domains define a conserved adenosine binding pocket. J. Virol. 83, 6534–6545.
[23] Egloff, M.P. et al. (2006) Structural and functional basis for ADP-ribose and poly(ADP-ribose) binding by viral macro domains. J. Virol. 80, 8493–8502.